# A Physics-Based Empirical Pseudopotential Model for Calculating Band Structures of Simple and Complex Semiconductors

Gary Pennington, Neil Goldsman, James M. McGarrity†, and Frank Crowne†
Department of Electrical Engineering, University of Maryland, College Park, MD 20742
Email: garyp@glue.umd.edu, neil@glue.umd.edu Fax:+1-301-3149281 Phone:+1-301-405-3648

† U.S. Army Research Laboratory
2800 Powder Mill Road, Adelphi, MD 20783

## I. INTRODUCTION

The full zone band structure is often needed for adequate simulation of semiconductor devices. It is important for devices operating under high-power, high-fields and determines many material properties. The computational ease and good accuracy of the empirical pseudopotential method (EPM) make it the bandstructure method of choice for full-zone simulations. While the EPM works well for most diamond and zincblende semiconductors, it becomes less effective for more complicated structures with larger unit cells. For these materials, more EPM parameters must be fit while less experimental data is usually avaliable. Through the adaption of the nonlocal atomic model potential of Heine and Animalu[1], we have developed a model empirical pseudopotential which, by drastically reducing the fitting parameters needed, can extend the use of the EPM to semiconductors with large unit cells. The method is effectively applied to the band structure calculations of Si, C, 3C-SiC, 4H-SiC, and 6H-SiC here.

## II. MODEL

Heine and Animalu (HA) developed a nonlocal model atomic potential which under a local approximation, successfully predicted the long wavelength form factors for many metals[1], [2]. The unscreened core potential was represented as a sum of angular-momentum-dependent, and thus nonlocal, square wells of depth $A_l$, each with the same radius $R$. These parameters were then fitted to the experimental energy levels of the corresponding free ions and then adjusted appropriately to account for energy scale changes in the metal. An approximation to the metal values was thus obtained by fitting to atomic spectroscopic data.

To use this model to represent the empirical pseudopotential, which is truncated in reciprical lattice vector ($\vec{q}$) space, the Fourier transform of the potential is damped according to

$$V(\vec{k}, \vec{q}) = V_{HA}(\vec{k}, \vec{q}) e^{-\alpha \Theta(x) x} \qquad (1)$$

Where $\vec{k}$ is the electron wavevector and $x = \left( \frac{|\vec{q}|}{2.2 k_f} - 1 \right)$

and

$$\Theta(x) = \begin{cases} 1 & x \geq 0 \\ 0 & x < 0 \end{cases} \qquad (2)$$

As appropriate for semiconductors[3], the damping factor $\alpha$ is adjusted so that the potential damps to zero for $q > 3k_f$, where $k_f$ is the Fermi wavevector, and the step function ensures that all truncation occurs well after $q = 2k_f$. This simple non-parameterized damping factor is chosen so that no new fitting parameters are introduced.

Other alterations of the potential are the use of an appropriate dielectric function for semiconductors[4], and for heteropolar semiconductors, the addition of a screened charge transfer $\Delta Z$. For an $A^{Z_A} B^{8-Z_B}$ compound, this is estimated from the asymmetric charge coefficent $g$[5] according to

$$g \simeq \frac{(8 - Z_A + \Delta Z \overline{\epsilon(q)}) - (Z_B - \Delta Z \overline{\epsilon(q)})}{8} \qquad (3)$$

Where $Z$ are the valences and the screened charge transfer is scaled by $\bar{\epsilon}$, the average of the dielectric function used. A screened charge transfer is used since it has been used[6] effectively to predict ionicity in numerous semiconductors without first row elements.

With these changes the atomic model potential, showing the model parameters used, for a C atom in a cubic semicondutor SC becomes

$$V_C^{sc} = \left[ \frac{B_C(q; A_{c2}, Z_C - \Delta Z_{sc}, R_c) + I_C(q; \Delta A_{c1}, R_c)}{\epsilon_{sc}(q)} \right. $$
$$\left. + F_C(\vec{k}, \vec{q}; \Delta A_{c1}, A^{NL}, R_c) \right] \frac{\Omega_c}{\Omega_{sc}} e^{-\alpha_{sc} \Theta(x) x} \qquad (4)$$

In this work SC may be either C, 3C-SiC, or, as will be discussed later in this section, an effective cubic potential for the hexagonal polytypes. The potential is scaled by the ratio of unit cell volumes $\Omega$, and damped as previously mentioned. The local, or $\vec{k}$ independent, bare potential $B$ is constructed from a local approximation to the $l=2$ square well plus the potential due to the net core charge ($+Z_c - \Delta Z_{sc}$). $F$ is the nonlocal bare core potential involving a square well of depth $\Delta A_{c1} = A_{c1} - A_{c2}$. Only

TABLE I

Model parameters in a.u. Fitting parameters indicated with (*).

|  | Si | C | 3C | 4H | 6H |
|---|---|---|---|---|---|
| $A_{Si0}$ | 2.08 |  | 2.08 | 2.08 | 2.08 |
| $A_{Si2}$ | 2.40* |  | 2.40 | 2.40 | 2.40 |
| $R_{Si}$ | 2.00 |  | 2.00 | 2.00 | 2.00 |
| $A_{C1}$ |  | 4.48 | 4.48 | 4.48 | 4.48 |
| $A_{C1}^{NL}$ |  |  | 0.3* | 0.4* |  |
| $A_{C2}$ |  | 3.94* | 4.06* | 3.90* | 3.93* |
| $R_C$ |  | 1.44 | 1.44 | 1.44 | 1.44 |
| $\Delta Z$ | 0 | 0 | 1 | 1 | 1 |

the $l=1$ well, representing the attractive potential due to the lack of p electrons in the core, is retained since it is the only well that differs significantly in depth from the $A_2$ well.

Following the work of HA, the "on Fermi sphere" method is used to take out the $\vec{k}$ dependence and approximate $F$ as a local function $F^L$, but a nonlocal correction $F^{NL}$ is also added to fine tune the bandstructures by fitting the effective masses to experiment.

$$F_c = F_c^L(q; A_{C1} - A_{C2}, R_c) + F_c^{NL}(\vec{k}, \vec{q}; A_{C1}^{NL}, R_c) \quad (5)$$

A potential similar to (1) can be constructed for Si atoms except that only the repulsive $l=0$ nonlocal core potential varies from $A_{Si2}$ and the charge transfer increases the net core charge to $(+Z_{Si} + \Delta Z_{SC})$. With these changes, the C and Si atomic potentials within C, Si, and 3C-SiC are obtained. For the hexagonal SiC polytypes, the wavevectors are scaled and effective cubic atomic potentials constructed so that the cubic parameters may be used as a first approximation to the hexagonal parameters.

To complete the Fourier transform of the unit cell potential, the Si and C potentials are multiplied by appropriate structure factors $S_{SC}^C$ and $S_{SC}^{Si}$. Summing over recprical lattice vectors, the potential of semiconductor SC is then

$$V_{SC}(\vec{r}) = \sum_{\vec{q}} \left[ V_C^{SC}(\vec{k}', \vec{q}) S_C^{SC}(\vec{q}) + V_{Si}^{SC}(\vec{k}', \vec{q}) S_{Si}^{SC}(\vec{q}) \right] e^{i\vec{q}\cdot\vec{r}} \quad (6)$$

SC may be Si(no C atoms used), C(no Si atoms used), or one of the SiC polytypes considered. For the hexagonal polytypes the primed wavevectors allow cubic potentials to be used. These electron and recprical lattice wavevectors are placed in cubic lattice vector units according to $\vec{k}'(\vec{q}') = \frac{a_{SC}}{a_{SCcubic}} \vec{k}(\vec{q})$, where $a_{SC}$ is the hexagonal and $a_{SCcubic}$ the cubic phase lattice constant. This takes into account differences in the density of wavevectors in the polytypes. Further differences in the bandstructure are accounted for by fitting of the parameters. For heteropolar semiconductors such as the SiC polytypes considered here, the potential can then be conveniently reorganized

TABLE II

Comparision Of Model Potential Band energies with Experiment

| Model | Expt. |  | Model | Expt. |
|---|---|---|---|---|
| **Si** | | | | |
| $E_{gap}$ 1.10 | 1.12[a] | $L_{3c}$ | 4.16 | 3.91[a] |
| $\Gamma_{1v}$ -12.52 | -12.56[a] | $L_{1v}$ | -7.24 | -6.82[a] |
| $\Gamma_{15c}$ 3.56 | 3.35[a] | $L_{3v}$ | -1.22 | -1.22[a] |
| $\Gamma_{2c}$ 4.04 | 4.16[a] | $L_{2v}$ | -10.17 | -9.34[a] |
| $L_{1c}$ 2.09 | 2.05[a] | $X_{4v}$ | -2.94 | -2.90[a] |
| **3C-SiC** | | **C** | | |
| $X_{1c}$ 2.30 | 2.39[b] | $E_{gap}$ | 5.50 | 5.51[c] |
| $X_{3c}-X_{1c}$ 2.74 | 3.10[d] | $\Gamma_{1v}$ | -28.47 | -21.00[e] |
| $\Gamma_{1c}$ 5.73 | 6.0[b] | $\Gamma_{15c}$ | 7.12 | 7[f](6[e]) |
| $L_{1c}$ 3.95 | 4.20[b] | $\Gamma_{2c}$ | 10.66 | 15.35[e] |
| $X_{1c}-L_{3v}$ 4.33 | 3.55[b] | $L_{1v}$ | -15.85 | -12.83[e] |
| **4H-SiC** | | **6H-SiC** | | |
| $E_{gap}$ 3.20(M) | 3.26[g](M) | | 3.00(L) | 3.02[g](M-L) |

Unless a difference in two band energies is indicated, all band energies are relative to the valence band maximum at $\Gamma$.

[a] Reference 7
[b] Reference 8
[c] Reference 9
[d] Reference 10
[e] Reference 11
[f] Reference 12
[g] Reference 13

in terms of symmetric and asymmetric potentials as in the EPM.

## III. RESULTS

For C and Si, with the exception of the carbon core radius $R_C$ which was chosen 4% less than the HA result, the HA results were used for the first approximation of the model parameters. One parameter, $A_2$, was then adjusted to fit the local model potential to experimental band energies of Si and C. For C, $A_{C2}$ was increased from the HA value by 21%, while for Si, $A_{Si2}$ was decreased by less than 2%. For all the semiconductors considered, the model parameters used are shown in Table I, plots of the bandstructure along symmetry lines of the Brillion zone are displayed in Fig. 1-5, and comparison with experimental band energies is made in Table II. For Si agreement with experiment is very good but for C, the results deviate away from the bandgap. Similar results for C have been attained using the EPM[12] and are primarily due to the weakness of local approximations to the strong nonlocal $l=1$ core potential. The potential is adequate for device simulations though, where the region of interest is primarily close to the bandgap.
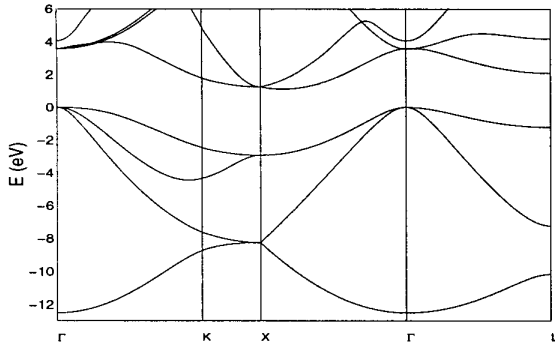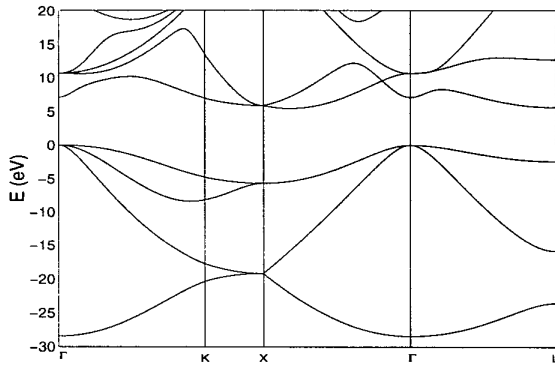
Fig. 1. Si model bandstructure
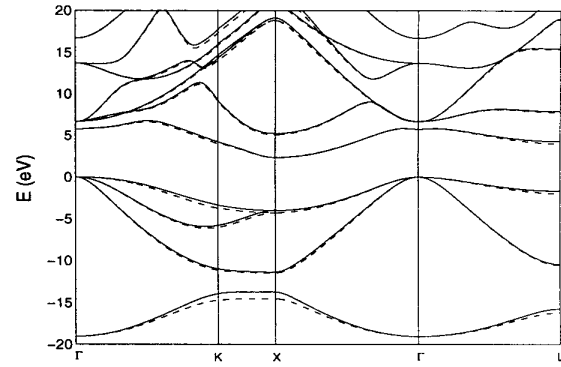


Fig. 2. C model bandstructure



Fig. 3. Local(-) and nonlocal(- -) 3C-SiC model bandstructure

TABLE III

Comparision Of Model Potential Effective Masses with Experiment

| | 3C-SiC | 4H-SiC | 6H-SiC |
|---|---|---|---|
| $m_1^*$(model) | $0.24 \pm 0.02$(XW) | $0.60 \pm 0.05$(M$\Gamma$) | $0.90 \pm 0.03$(LA) |
| $m_1^*$(exp.) | $0.247^a$(XW) | $0.58^b$(M$\Gamma$) | |
| $m_2^*$(model) | $0.24 \pm 0.02$(XW) | $0.20 \pm 0.02$(MK) | $0.22 \pm 0.02$(LH) |
| $m_2^*$(exp.) | $0.247^a$(XW) | $0.29^b$(MK) | |
| $m_3^*$(model) | $0.70 \pm 0.06$(X$\Gamma$) | $0.36 \pm 0.02$(ML) | $1.43 \pm 0.02$(LM) |
| $m_3^*$(exp.) | $0.667^a$(X$\Gamma$) | $0.33^b$(ML) | |
| $m_\perp^*$ (model) | | $0.35 \pm 0.02$ | $0.44 \pm 0.02$ |
| $m_\perp^*$ (exp.) | | $0.42^c$ | $0.42^c$ |
| $m_\parallel^*$(model) | | $0.31 \pm 0.05$ | $1.14 \pm 0.14$ |
| $m_\parallel^*$(exp.) | | $0.29^c$ | $2.0 \pm 0.2^c$ |

[a]Reference 15
[b]Reference 16
[c]Reference 17

For the SiC polytypes, the charge transfer $\Delta Z_{SiC}$ was included and all of the Si and C local potential parameters were retained as a first approximation. Local bandstructures were then obtained by slightly adjusting $A_{C2}$ by 3% or less to fit the bandstructure to experiment. Since the effective masses for 3C and 4H were significantly larger than experiment along the direction towards the center of the Brillouin zone, nonlocal corrections were included, introducing a second fitting parameter $A_{C1}^{NL}$. This also involved a slight readjustment of $A_{C2}$ in 4H. The conduction band minima, found at $X$ in 3C, $M$ in 4H, and $L$ in 6H, agree well with experiment[8], [13]. In density function theory bandstructures[14], [15], the 6H minimum is usually found closer to the $M$ point along $M$-$L$, but as found here the lowest conduction band is extremely flat along $M$-$L$, varing by less than .1eV. The model potential results are consistent with experiment[16] though since the exact postion of the minimum along the $M$-$L$ symmetry line has not been determined.

Comparison with experimental effective masses is made in Table III. A large longitudinal mass and a smaller transverse effective mass relative to the $X$-$\Gamma$ direction are found for 3C, agreeing with experiment. Greater anisotrophy is found for the hexagonal polytypes. For 4H, a large mass is found along $M$-$\Gamma$, while smaller yet clearly distinct masses are found in the transverse directions. Agreement with experiment is good except for a slightly lower fitted mass along the $M$-$K$ direction. For 6H an extremely large effective mass is found along the $L$-$M$ direction. The mass along $L$-$H$ is quite small while the mass along $L$-$A$ is large but still much smaller than the in $L$-$M$ mass.

The experimental values of $m_\perp$ and $m_\parallel$ in Table III were obtained by experiments[19] in which variations in the effective mass as determined for magnetic fields in the plane perpendicular to the c direction where not resolved. These "in-plane invariant"[18] effective masses were then approximated from the model bandstructure for comparison. For 6H, $m_\perp$ is fitted well, whereas $m_\parallel$ is found to be much lower than experiment. This may result from band filling complications due to the flat bandstructure along $M$-$L$. The 6H masses although are found to be consistant with work done using density function theory[18].
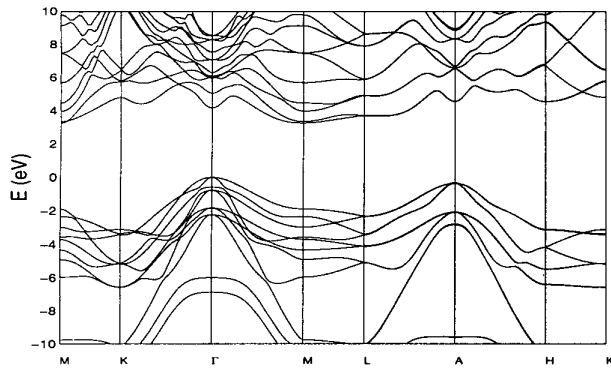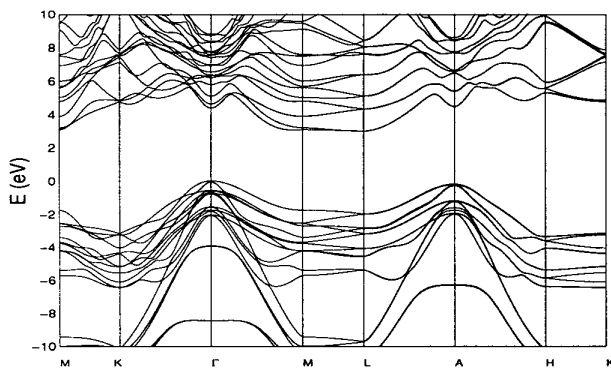
Fig. 4. 4H-SiC model bandstructure



Fig. 5. 6H-SiC model bandstructure

## IV. CONCLUSION

By fitting one parameter in the HA potential and adding charge transfer we are able to attain a local model potential which can be brought to agreement with experimental data for Si, C(around the bandgap), and the SiC polytypes. This potential is amended by a nonlocal correction to fine tune the bandstructures if necessary, and is used to fit the SiC effective masses to experiment. The model allows the extentsion of the EPM to materials where many more form factors parameters are need than avaliable data. The model can be attained for increasingly complex unit cells through transferability. This is demonstrated by the use of essentially the same potentials in Si and C for the SiC polytypes considered, with slight adjustment of one fitting parameter to account for changes in the potential.

REFERENCES

[1] A. O. E. Animalu and V. Heine, "Screened model potential for 25 elements," *Phil. Mag.*, vol. 12, pp. 1249-1269, 1965.

[2] A. O. E. Animalu, "The total electronic band structure energy for 29 elements," *Proc. Roy. Soc. A*, vol. 294, pp. 376-392, March 1966.

[3] M. L. Cohen and V. Heine, "The fitting of pseudopotentials to experimental data and their subsequent application," in *Solid State Physics*, vol. 24, Acedemic press, 1970, pp. 38-246.

[4] D. R. Penn, "Wave-number-dependent dielectric function of semiconductors," *Phy. Rev.*, vol. 128, pp. 2093-2097, December 1962.

[5] A. Garcia and M. L. Cohen, "First-principles ionicity scales. I. Charge asymmetry in the solid state," *Phy. Rev. B*, vol. 47, pp. 4212-4220, February 1992.

[6] F. Aymerich, R. Meloni, and G. Mula, "General model pseudopotential: Binary compounds," *Phy. Rev. B*, vol. 15, pp. 3980-3985, April 1977.

[7] D. R. Masovic, F. R. Vukajlovic, and S. Zekovic, "Local-pseudopotential calculation for optical properties and photoemission valence-band spectrum of silicon," *J. Phys. C*, vol. 16, pp. 6731-6738, December 1983.

[8] W. J. Choyke and L. Patrick, "Higher absorption edges in cubic SiC," *Phy. Rev.*, vol. 187, pp. 1041-1043 November 1969.

[9] L. Patrick and W. J. Choyke, "Optical absorpton in n-type cubic SiC," *Phy. Rev.*, vol. 186, pp. 775-777, October 1969.

[10] F. J. Himpsel, J. F. van der Veen, and D. E. Eastman, "Experimental bulk energy bands for diamond using hv-dependent photoemission," *Phy. Rev. B*, vol. 22, pp. 1967-1971, August 1980.

[11] F. J. Himpsel, J. A. Knapp, J. A. van Vechten, and D. E. Eastman, "Quantum photoyield of diamond(111), a stable negative-affinity emitter," *Phy. Rev. B*, vol. 20, pp. 624-627, July 1979.

[12] L. A. Hemstreet, C. Y. Fong, and Marvin L. Cohen, "Calculation of the band structure and optical constants of diamond using the nonlocal-pseudopotential method," *Phy. Rev. B*, vol. 2, pp. 2054-2063, September 1970.

[13] W. J. Choyke, D. R. Hamilton, and L. Patrick, "Optical properties of cubic SiC: Luminescence of nitrogen-exciton complexes, and interband absorption," *Phy. Rev.*, vol. A133, pp. A1163-A1166, February 1964.

[14] C. H. Park, B. Cheong, K. Lee, and K. J. Chang, " Structural and electronic properties of cubic, 2H, 4H, and 6H SiC, " *Phy. Rev. B*, vol. 49, pp. 4485-4493 , October 1993.

[15] W. R. L. Lambrecht, S. Limpijumnong, S.N. Rashkeev, and B. Segall, "Electronic band structure of SiC polytypes: A discussion of theory and experiment," *Phys. Stat. Sol. B*, vol. 202, pp. 5-33 , May 1997.

[16] L. Patrick, "Konh-Luttinger interference effect and location of the conduction-band minima in 6H SiC," *Phys. Rev. B*, vol. 5, pp. 2198-2206, March 1972.

[17] R. Kaplan and R. J. Wagner, "Electron cyclotron resonance in cubic SiC," *Solid State Communications*, vol. 55, pp. 67-69 February 1985.

[18] W. R. L. Lambrecht and B. Segall, "Band-structure analysis of the conduction-band mass anisotropy in 6H and 4H SiC," *Phy. Rev. B*, vol. 52, pp. 2249-2252, July 1995.

[19] N. T. Son et al., "Electron effective masses in 4H SiC," *Appl. Phys. Lett.*, vol. 66, pp. 1074-1076 , February 1995.